Journal of Statistical Physics, Vol. 59, Nos. 1/2, 1990

The Nearest-Neighbor Resonating-Valence Bond State in a Grassmannian Form

Thomas Blum[1] **and Yonathan Shapir**[1,2]

Received July 28, 1989

The nearest-neighbor resonating-valence bond (NNRVB) state is studied using classical anticommuting (Grassmann) variables. The classical partition function corresponding to the self-overlap of the NNRVB wavefunction is generated from a local (bond) Hamiltonian expressed in terms of four anticommuting variables. It is shown that the one-particle-per-site constraint introduces an interaction term which is a local product of all four variables. Two approaches are applied to study this Hamiltonian: (i) a self-consistent field decoupling scheme and (ii) a systematic perturbation expansion around the unconstrained soluble point. Bounds on the norm of the wavefunction are derived. Extensions to the presence of holes, long-range valence bonds, and the introduction of phase fluctuations [which violate the Marshall sign rule and yield a $U(1)$ gauge theory] are discussed.

KEY WORDS: Grassmann Variable; Hubbard model; Heisenberg antiferromagnet (AF); resonating valence bond (RVB) state.

1. INTRODUCTION

The desire to uncover the mechanism behind the high-T_c superconductors has renewed interest in two long-standing problems—namely the two-dimensional ($2D$) Hubbard model and the $2D$ Heisenberg antiferromagnet (AF). In different limits, the Hubbard model can describe both nonmagnetic metals and AF insulators. Its Hamiltonian is given by

$$H_{\text{Hubbard}} = -\sum_{\langle ij \rangle} \sum_{\sigma} t_{ij}(c_{i\sigma}^{+} c_{j\sigma} + c_{j\sigma}^{+} c_{i\sigma}) + \sum_{i} U n_{i\uparrow} n_{i\downarrow} \tag{1}$$

[1] Department of Physics and Astronomy, University of Rochester, Rochester, New York 14627-0011.

[2] Department of Physics, The Technion-IIT, 32000 Haifa, Israel.

0022-4715/90/0400-0333$06.00/0 © 1990 Plenum Publishing Corporation

where $c_{i\sigma}^{+}$ ($c_{i\sigma}$) creates (annihilates) an electron of spin σ at site i, t_{ij} is the tunneling matrix element, and U is the on-site Coulomb repulsion energy. It is widely believed that the Hubbard model (near half-filling and with moderately large U) captures the essential features of these superconducting materials.[1-6] In turn, the corresponding undoped Mott insulators (such as La_2CuO_4) would be describable by the large-U, half-filled Hubbard model. In this limit second-order perturbation theory yields a Hamiltonian which behaves effectively as a Heisenberg AF:

$$H_{\text{Heisenberg}} = -J \sum_{\langle ij \rangle} \mathbf{S}_i \cdot \mathbf{S}_j \tag{2}$$

where $J \simeq -4t^2/U$ and t_{ij} is nonzero only when i and j are nearest neighbors. Allowing small nonzero next-nearest-neighbor values of t_{ij} would lead to a frustrated Heisenberg AF. This problem has also received much attention lately.[1,6]

Compared to its classical counterpart, a quantum spin system is complicated not only by quantum fluctuations, but also by symmetry considerations. Quantum fluctuations play a major role in the problem at hand because both the spin and the dimension are low. Furthermore, whereas the symmetry properties of the ferromagnet's ground state are simple, those of the AFs ground state are highly nontrivial. A standard approach to the Heisenberg AF involves spin-wave theory, which includes, e.g., the Holstein–Primakoff transformation[7] and its expansion in terms of AF (or Néel) magnons.[8,9] The approximation is justifiable for large values of the spin and in higher dimensions; however, the problem at hand involves spin 1/2 and is only 2D. Moreover, alternative methods such as the path integral technique seem to indicate topological differences between integral and nonintegral spin (at least in 1D)[10]—a distinction not brought out by the usual spin wave expansions. Consequently, alternate possibilities warrant attention.

One choice is the resonating-valence bond (RVB) state. Anderson proposed the RVB state first in the context of frustrated Heisenberg AFs[11] such as that on a triangular lattice and later conjectured its role in high-T_c superconductivity.[1] Bethe's exact solution in one dimension[12] and Hulthèn's cluster approach[13] motivated Anderson to construct a liquidlike state comprised of spins paired into singlets with the system resonating between all the possible configurations. The coherent resonances can lead to long-range order AF in some versions of the RVB state.[14-16] A small frustrating term, whether it be due to next-nearest-neighbor tunneling matrix elements or to the introduction of holes, may tend to benefit the RVB state over a Néel-like state.

The main problem the RVB state presents is calculational difficulty.

This is largely due to the fact that states corresponding to different configurations are not orthogonal. Various versions of and approaches to the RVB have been pursued. Some works have studied mean-field BCS-like approaches.[2–5] These may exhibit the possible order parameters and the conditions for their condensation; however, they involve the strong "real-space" constraint which allows only one particle per site. The Gutzwiller projection operation (or alternative methods such as the slaved bosons approach) leads to new complications not present in weak-coupling theories such as BCS. Others have chosen to consider real-space dimer-like approaches.[17–19] The real-space approaches avoid the difficulty of inserting the constraint by taking it into account from the outset. In view of the short-ranged pairing in copper oxides, this approach seems worthy of further exploration.

Among the real-space approaches, we concentrate on the one introduced by Sutherland.[17] In this version only nearest-neighbor spins are paired into singlets (NNRVB). In order to construct the NNRVB state, first consider a dimer covering (called a) of a bipartite lattice. Each dimer connects two nearest neighbor sites—one on each sublattice. The spins associated with each dimer form a singlet state:

$$\phi(i, j) = |\uparrow_i \downarrow_j\rangle - |\downarrow_i \uparrow_j\rangle \tag{3}$$

where the first site (i) is on sublattice A and the second (j) is on sublattice B. Maintaining this convention is important for producing a state that will obey the Marshall sign "rule."[20] Next, let the "singlet pair state" $|a\rangle$ be defined as the product of all such singlet states on a given dimer covering (a):

$$|a\rangle = \prod_{\langle ij\rangle \in a} \phi(i, j) \tag{4}$$

Finally, the NNRVB wavefunction is the (coherent) linear superposition of these wavefunctions associated with all possible dimer configurations:

$$|\psi\rangle = \sum_a |a\rangle \tag{5}$$

Though easily constructed, the NNRVB state remains difficult to utilize in calculations. Since each singlet pair state $|a\rangle$ contains the two AF states, different singlet pair states $|a\rangle$ and $|b\rangle$ are not orthogonal. In fact, $|a\rangle$ and $|b\rangle$ will in general have even more states in common. However, as suggested by Sutherland,[17] many of the properties of the RVB wavefunction may be deduced from its self-overlap:

$$\langle\psi|\psi\rangle = \sum_{\{a,b\}} \langle a|b\rangle \tag{6}$$

which may be expressed as the partition function of a classical model

$$\langle \psi | \psi \rangle = Z(2, 4) = \sum_{\{C\}} 2^{p_2} 4^{p} \tag{7a}$$

The sum includes all close-packed coverings of the lattice by double dimers (or degenerate loops) and loops; p_2 indicates the number of double dimers and p the number of loops. A factor of two is associated with each double dimer and a factor of four with each loop. Note that the very definition of NNRVB used above and the map to $Z(2, 4)$ necessitate that the underlying lattice be bipartite. Our approach cannot be applied to frustrated versions of the problem; in general, it requires that the Marshall sign rule hold. It is convenient to consider $Z(2, 4)$ as a special case of the more general partition function $Z(x, y)$[21,22]

$$Z(x, y) = \sum_{\{C\}} x^{p_2} y^{p} \tag{7b}$$

Some works have pursued a study of the $SU(n)$ generalization of the Heisenberg AF in the large-n limit.[3,16,23] As n increases, the amount of quantum fluctuation decreases. This is reflected in the fact that up to order $1/n$, the singlet pair states $|a\rangle$ and $|b\rangle$ are orthogonal. The corresponding NNRVB self-overlap in the $SU(n)$ AF is $Z(n, 2n)$ [or written in terms of the spin s it is $Z(2s+1, 4s+2)$]. As n increases, configurations with even the smallest of loops decrease in importance and the dimer configurations dominate the partition function. Therefore, to the first order in $1/n$, one must only consider dimer configurations and configurations containing a single loop the size of a plaquette. In this limit, the NNRVB state becomes more "spin-Peierls"-like and less Néel-like.[23,24]

In a recent work, Shapir and Kohmoto[19] derived a classical Hamiltonian which generates the required dimer-loop configurations. The associated field theory, an $O(4)$ model in a logarithmic potential, was found from a Hamiltonian comprised of local (bond) contributions. They employed commuting variables on which special trace rules had to be imposed in order to satisfy the hard-core constraints. A mean-field estimate for $Z(2, 4)$ was found. In addition, they related the AF correlations to the energy–energy correlations of the classical model and showed them to be short-ranged in 2D if only nearest neighbor singlets were allowed. (The interesting question that remains is: What is the behavior of the dimer–dimer correlations?) The local triplet excitations were analyzed by the Feynman–Bijl approach and were shown to have a finite energy gap.

There are certain advantages to having an anticommuting real-space representation in addition to this commuting one. For example, the usual

fermionic constraint preventing multiple occupation of a site by identical particles is automatically included in the anticommuting formulation, and a one-particle-per-site constraint is easily imposed. Moreover, the fermionic nature is likely to influence the statistics of the excitations once the system is diluted away from half-filling. Also, the connection between real-space and momentum-space approaches is more apparent in this representation. As in many other 2D models, the bosonic and the fermionic pictures, though equally applicable, complement each other by illuminating different aspects of the whole picture.

The description of $Z(2, 4)$ in terms of either commuting or anticommuting classical variables is similar to the case of 1D quantum spin systems with nearest neighbor interactions, which can be formulated in terms of either hard-core bosonic operators or (spinless) fermionic operators. In fact, in that case one representation can be directly transformed into the other via the Jordan–Wigner transformation.[25,26] When the Jordan–Wigner transformation is applied to the 2D quantum spin system, it produces nonlocal effects. It can lead to couplings with phase factors which depend on a summation of number operators (along a "string"). However, the large-U and half-filled limits may place enough restriction on the number operators to trivialize the phase factor and consequently allow both fermionic and bosonic representations. But as one moves away from these limits, the simple correspondence between the treatments would be lost. Recently, Fradkin introduced a generalized (multivalued) Jordan–Wigner transformation[27] to investigate a mapping between a 2D lattice gauge field theory with a Chern–Simons term and the 2D spin-1/2 XY model.

In Section 2 we introduce a systematic Grassmannian representation to the self-overlap of the NNRVB state (which was briefly outlined elsewhere[28]). A real-space expansion technique shows that it produces the correct configurations with the appropriate weights and signs. In Section 3, we offer two schemes for approximating the self-overlap. The first is a self-consistent decoupling scheme and the second a perturbative expansion (in momentum space). We also provide upper and lower bounds on the self-overlap. In Section 4, we discuss the $U(1)$ gauge theory obtained when phase fluctuations are allowed. In addition, we examine the introduction of holes and their statistics. In Section 5, we recapitulate our results, compare them with the results of others, and outline our future plans regarding this representation. A systematic approach to calculating $Z(2, 4)$ on strips of finite widths is presented in the Appendix.

2. THE GRASSMANNIAN REPRESENTATION

To represent the two spin states of each particle we introduce two pairs of Grassmann variables: η_i^*, η_i and ξ_i^*, ξ_i, which all anticommute with one another. The product $\eta_i^*\eta_i$ (or $\xi_i^*\xi_i$) will indicate the presence of an electron with one (or the other) definite spin state. Note, however, that they do not represent spin up (or down), but rather the two possible AF ground states. In other words, $\eta_i^*\eta_i$ represents spin up on one sublattice and spin down on the other one and vice versa for $\xi_i^*\xi_i$.

To implement the constraint of one particle per site of the large-U Hubbard system at half-filling, we modify the definition of the Grassmannian integration[3] to include a "Gutzwiller projector." For any function $f(\eta^*, \eta, \xi^*, \xi)$ we define

$$\int Dg f(\eta^*, \eta, \xi^*, \xi) = \int \prod_j [d\eta_j^*\, d\eta_j\, d\xi_j^*\, d\xi_j (\eta_j\eta_j^* + \xi_j\xi_j^*)]\, f(\eta^*, \eta, \xi^*, \xi) \tag{8}$$

Two particles on the site j would be represented by $\eta_j^*\eta_j\xi_j^*\xi_j$ arising from f; while no particles (a hole) would be represented by 1. However, both of these possibilities are eliminated by the projector $\eta_j^*\eta_j + \xi_j^*\xi_j$ in the integration measure.

Using this measure, the self-overlap $\langle\psi\,|\,\psi\rangle$ becomes

$$\langle\psi\,|\,\psi\rangle = Z(2, 4) = \int Dg \exp[H(\eta^*, \eta, \xi^*, \xi)] \tag{9}$$

where

$$H(\eta^*, \eta, \xi^*, \xi) = \sum_j (\eta_j^*\eta_{j+e_x} + \eta_j\eta_{j+e_x}^* + i\eta_j\eta_{j+e_y} + i\eta_j^*\eta_{j+e_y}^* + \{\eta \to \xi\}) \tag{10a}$$

The factor of i associated with the vertical bonds makes this formulation closely related to the $s+id$ phase introduced by Kotliar.[4] Other expressions for $H(\eta^*, \eta, \xi^*, \xi)$ lead to the same classical partition function; for example,

$$H(\eta^*, \eta, \xi^*, \xi) = \sum_j (\eta_j^*\eta_{j+e_x} + \eta_j\eta_{j+e_x}^* + (-1)^{j_x}\eta_j^*\eta_{j+e_y} + (-1)^{j_x}\eta_j\eta_{j+e_y}^* + \{\eta \to \xi\}) \tag{10b}$$

[3] See ref. 29 for definitions and applications to other models in statistical mechanics.

and

$$H(\eta^*, \eta, \xi^*, \xi) = \sum_j (e^{i\pi/4}\eta_j^*\eta_{j+e_x}^* - e^{-i\pi/4}\eta_j\eta_{j+e_x} - e^{-i\pi/4}\eta_j^*\eta_{j+e_y}^* + e^{i\pi/4}\eta_j\eta_{j+e_y} + \{\eta \to \xi\}) \quad (10c)$$

But note that none of these Hamiltonians is symmetric under rotation by $\pi/2$. Expressions (10a) and (10c) have the advantage that the couplings do not depend on position; while (10b) has all terms of the same form (including the projector). As with the commuting representation, there is a symmetry between η's and η^*'s (likewise ξ's and ξ^*'s) as well as one between the pairs (η^*, η) and (ξ^*, ξ). These lead to the previously mentioned $O(4)$ symmetry.

The Grassmann representation of the NNRVB self-overlap is easily extendible to the $SU(n)$ generalization of the Heisenberg AF. Instead of two pairs of Grassmann variables, one would introduce n pairs.

In the (real-space) diagrammatic expansion of the partition function adapted from that of Samuel,[30] each pair of Grassmann variables is represented by an arrow pointing from the site of the first to that of the second. In addition, one finds attached to the ends of each arrow an **x** or an **o** corresponding to whether the variable represented is starred or unstarred. For example,

$$\eta_i^*\eta_j \text{ corresponds to } \mathbf{x} \to \mathbf{o}$$

Consequently, in the above Hamiltonian (10a), horizontal bonds always point in the positive x direction and attach **x**'s to **o**'s or **o**'s to **x**'s; while vertical bonds always point in the positive y direction and attach **x**'s to **x**'s or **o**'s to **o**'s. At each site two and only two bonds (one labeled **o**, the other **x**) must arise from the expansion. Thus, the only contributing configurations are close-packed arrangements of loops and (double) dimers. There are four possibilities ($\eta_i\eta_j^*$, $\eta_i^*\eta_j$, $\xi_i\xi_j^*$, or $\xi_i^*\xi_j$) for each bond in a loop; however, once one bond is selected, the remaining bonds in the loop are determined uniquely—hence the desired weight of four for loops. A similar argument yields two for (double) dimers.

Finding the sign associated with each diagram requires a little more thought. Consider the simple example of a square (see Fig. 1). One of the terms arising from the expansion is

$$h = \int Dg[\eta_a^*\eta_b][(i)\eta_c^*\eta_b^*][\eta_d^*\eta_c][(i)\eta_d\eta_a] \quad (11a)$$

Note that with every vertical bond comes an i; hence, a factor of $(i)^V$ arises, where V is the number of vertical bonds (V is always even). Next, consider

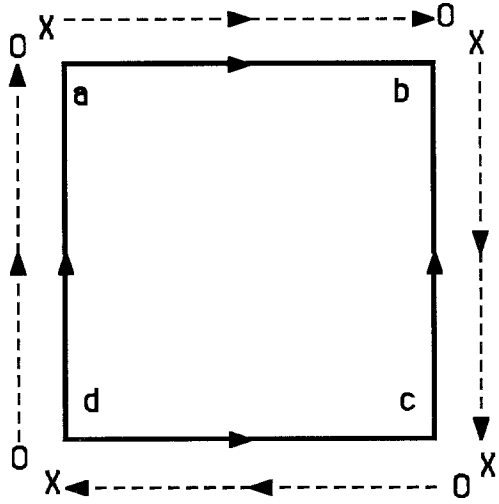

Fig. 1.

the diagram to be traversed in the clockwise direction. To facilitate the integration, switch all pairs not appearing in order traversed (except that corresponding to the first and the last terms in the expansion). Such a step requires exchanging only "bond" pairs and not "site" pairs. This operation introduces a term $(-1)^A$, where A is the number of bonds passed over against their assigned direction. Then note that the first and last terms in the expansion do not appear in the order traversed. Switching these brings in an additional (-1); this is the universal (-1) arising from fermion loops. Finally, the unstarred variable (at each site) should appear first. Making the appropriate exchanges here results in a factor of $(-1)^{XO}$, where XO is the number of times one encounters "XO" (as opposed to "OX") while progressing around the loop,

$$h = (-1)^{V/2 + A + XO + 1} \int Dg\, \eta_a \eta_a^* \eta_b \eta_b^* \eta_c \eta_c^* \eta_d \eta_d^*$$

$$= (-1)^{V/2 + A + XO + 1} \tag{11b}$$

In the case of the square in Fig. 1, $V/2$ is one, A is two, XO is two, and the overall sign is positive.

Next one can adopt an inductive method to show that any loop enclosing an even (odd) number of sites carries a positive (negative) weight. Consider a diagram containing the bond shown in Fig. 2a and consider changing it to the bonds in Fig. 2b. Such a replacement alters A by one, $V/2$ by one, and XO by two or zero, depending on the direction of

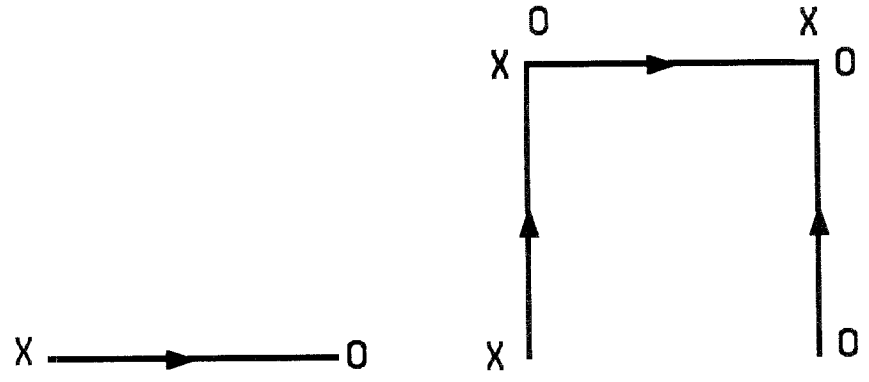

(a) (b)

Fig. 2.

traversal, but the overall sign of the diagram remains unaltered. Furthermore, the number of sites within the loop would remain the same or differ by two. Applying this result to the square, one finds that a rectangle of dimension two-by-one also has a positive weight, and so forth.

On the other hand, consider substituting the bonds in Fig. 3a with those in Fig. 3b. This step requires changing *XO* by one and hence flips the overall sign. In addition, it modifies the number of sites within the loop by one. Calculating a few simple diagrams such as the square and the double dimers and then tabulating the effect of extensions should convince one of the above-mentioned sign rule. In a close-packed gas of loops and double

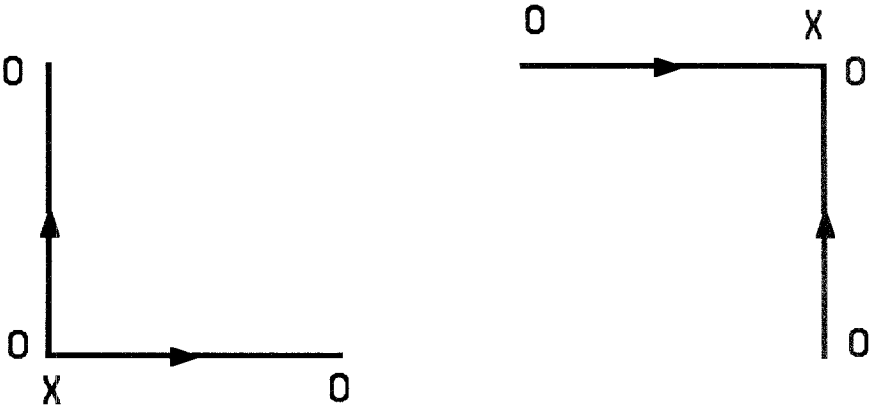

(a) (b)

Fig. 3.

dimers on a square lattice, no loop can enclose an odd number of sites, and so this sign rule presents no problem. However, eventually, we would like to consider the effect of holes and then this result becomes important.

3. APPROXIMATING THE SELF-OVERLAP $\langle\psi|\psi\rangle$

It is desirable to attempt to compute $Z(2, 4)$. First, the constraint (Gutzwiller projector) should be recast as an exponential, for instance, as

$$\prod_j (\eta_j^*\eta_j + \xi_j^*\xi_j) = \lim_{z\to\infty} \exp\left\{\sum_j [z(\eta_j^*\eta_j + \xi_j^*\xi_j) - z^2\eta_j^*\eta_j\xi_j^*\xi_j - \ln z]\right\} \tag{12}$$

Now the constraint can be made part of the Hamiltonian. Without the quartic (interactive) term, the integration would decouple into separate integrations, one over the ξ's and one over the η's, and both could be explicitly performed. Each integration would correspond to configurations of dimers, loops, and holes (with weights of z). Then, as z approaches infinity, holes would dominate all the configurations. The quartic term prevents this catastrophe, but in the process complicates the problem by coupling the integrations. Thus, we must find a way of dealing with these complexities. Most of the methods for treating an interactive (fermionic) field theory have a Grassmann variable version.[31] First, we will apply a decoupling scheme to the quartic term. Then we discuss a (momentum space) expansion in the quartic term.

3.1. A Decoupling Scheme for the Self-Overlap

Consider the decoupling scheme in which the term $\eta_j^*\eta_j\xi_j^*\xi_j$ is replaced by $\eta_j^*\eta_j\langle\xi_j^*\xi_j\rangle$. Such a scheme breaks the $\eta \to \xi$ symmetry. Let us examine the problem on an $L\times L$ lattice with L even; N $(=L^2)$ is the number of lattice sites. When periodic boundary conditions are applied, the system is translationally invariant; that is, $\langle\xi_j^*\xi_j\rangle$ is independent of j, and the operators are easily Fourier transformed. We have

$$\eta_j = L^{-1}\sum_k e^{i\mathbf{k}\cdot\mathbf{j}}a_k \qquad \text{and} \qquad \xi_j = L^{-1}\sum_k e^{i\mathbf{k}\cdot\mathbf{j}}b_k \tag{13}$$

where $\mathbf{k} = L^{-1}(2\pi s\hat{\mathbf{e}}_x + 2\pi t\hat{\mathbf{e}}_y)$, and

$$\frac{-(L-1)}{2} \leqslant s,\ t \leqslant \frac{L-1}{2}$$

The self-overlap $\langle\psi|\psi\rangle_{\text{dec}}$ is then given by

$$\begin{aligned}\langle\psi|\psi\rangle_{\text{dec}} = \lim_{z\to\infty} z^{-N} \prod_{k>0} \Big\{ \int da^*_{-k}\, da_{-k}\, da^*_k\, da_k \\ \times \exp[(2i\sin k_x + z - z^2\langle\xi^*\xi\rangle) a^*_k a_k \\ + (-2i\sin k_x + z - z^2\langle\xi^*\xi\rangle) a^*_{-k} a_{-k} \\ + 2\sin k_y\, a_k a_{-k} - 2\sin k_y\, a^*_k a^*_{-k}] \Big\} \\ \times \prod_{k>0} \Big\{ \int db^*_{-k}\, db_{-k}\, db^*_k\, db_k \\ \times \exp[(2i\sin k_x + z) b^*_k b_k + (-2i\sin k_x + z) b^*_{-k} b_{-k} \\ + 2\sin k_y\, b_k b_{-k} - 2\sin k_y\, b^*_k b^*_{-k}] \Big\} \end{aligned} \tag{14}$$

which leads to

$$\begin{aligned}\langle\psi|\psi\rangle_{\text{dec}} = \lim_{z\to\infty} z^{-N} \Big\{ \prod_{s>0}\prod_{t>0} \Big[(z - z^2\langle\xi^*\xi\rangle)^2 \\ + 4\sin^2\left(\frac{2\pi s}{L}\right) + 4\sin^2\left(\frac{2\pi t}{L}\right) \Big] \Big\}^2 \\ \times \Big\{ \prod_{s>0}\prod_{t>0} \Big[z^2 + 4\sin^2\left(\frac{2\pi s}{L}\right) + 4\sin^2\left(\frac{2\pi t}{L}\right) \Big] \Big\}^2 \end{aligned} \tag{15}$$

The self-consistency relation follows:

$$\begin{aligned}\langle\xi^*\xi\rangle_{\text{dec}} &= N^{-1}\sum_j \langle\xi^*_j\xi_j\rangle = N^{-1}\sum_k \langle b^*_k b_k\rangle \\ &= N^{-1}\sum_{s>0}\sum_{t>0} \left[\frac{4z}{z^2 + 4\sin^2(2\pi s/L) + 4\sin^2(2\pi t/L)} \right] \end{aligned} \tag{16}$$

In the limit as N approaches infinity, this becomes

$$\langle\xi^*\xi\rangle_{\text{dec}} = \frac{z}{\pi^2}\int_0^\pi dk_x \int_0^\pi dk_y\, [z^2 + 4\sin^2(k_x) + 4\sin^2(k_y)]^{-1} \tag{17}$$

An expansion in z^{-1} yields $\langle\xi^*\xi\rangle = z^{-1} - 4z^{-3}$. Substituting into the expression for the self-overlap and taking the limit as z approaches infinity, one obtains

$$\langle\psi|\psi\rangle_{\text{dec}} = \Big\{ \prod_{s>0}\prod_{t>0} \Big[4\sin^2\left(\frac{2\pi s}{L}\right) + 4\sin^2\left(\frac{2\pi t}{L}\right) \Big] \Big\}^2 = Z(1,2) \tag{18}$$

In this decoupling scheme $\langle\psi|\psi\rangle_{\text{dec}}$ equals $Z(1, 2)$. The decoupling scheme breaks the $\eta \to \xi$ symmetry and as a result all ξ's come from the measure, while all η's come from the expanded Hamiltonian (recall that $\langle \xi^* \xi \rangle$ approaches zero as z approaches infinity). Hence $Z(1, 2)$ need only involve one set of the variables and is easily solved. $Z(1, 2)$ can be shown to be the square of Z_{dimer} and the large-N limit was found by Kasteleyn.[32] It can be obtained by taking the logarithm and replacing the resulting sums by integrals. We have

$$\ln[Z(1, 2)] = N \ln 2 + 2 \sum_{s>0} \sum_{t>0} \ln \left[\sin^2 \left(\frac{2\pi s}{L} \right) + \sin^2 \left(\frac{2\pi t}{L} \right) \right] \tag{19a}$$

$$\ln[Z(1, 2)] = N \ln 2 - \frac{N}{4} \sum_{n=1}^{\infty} \frac{4^{-2n}}{n} \binom{2n}{n}^2 \tag{19b}$$

$$\ln[Z(1, 2)] = N \left(\frac{2G}{\pi} \right) \simeq N(0.5831) \tag{19c}$$

where G is Catalan's constant,

$$G = 1 - \frac{1}{3^2} + \frac{1}{5^2} + \cdots \simeq 0.9160 \tag{19d}$$

3.2. A Perturbative Expansion for the Self-Overlap

A second method for approximating the self-overlap involves a perturbative expansion around the soluble (noninteracting) point. If one Fourier transforms the system with the $\eta_j^* \eta_j \xi_j^* \xi_j$ terms included, the resulting expression is

$$\begin{aligned} \langle\psi|\psi\rangle = \lim_{z \to \infty} z^{-N} \int \prod_k da_k^* \, da_k \, db_k^* \, db_k \\ \times \exp \Bigg\{ \sum_k \left[(2i \sin k_x + z)(a_k^* a_k + b_k^* b_k) \right. \\ \left. + i e^{-ik_y} (a_k a_{-k} + b_k b_{-k}) + i e^{ik_y} (a_k^* a_{-k}^* + b_k^* b_{-k}^*) \right] \\ - \frac{z^2}{N} \sum_k \sum_p \sum_q a_k^* a_p b_q^* b_{k+q-p} \Bigg\} \end{aligned} \tag{20}$$

Again, if it were not for the last term, the integration could easily be done. An expansion in the last term yields

$$\langle\psi|\psi\rangle = \lim_{z\to\infty} z^{-N} \int \prod_k da_k^* \, da_k \, db_k^* \, db_k$$
$$\times \left[\prod_k \prod_p \prod_q (1 + \lambda a_k^* a_p b_q^* b_{k+q-p})\right]$$
$$\times \exp\left\{\sum_k [(2i \sin k_x + z)(a_k^* a_k + b_k^* b_k)\right.$$
$$\left. + ie^{-ik_y}(a_k a_{-k} + b_k b_{-k}) + ie^{ik_y}(a_k^* a_{-k}^* + b_k^* b_{-k}^*)]\right\} \quad (21)$$

where $\lambda = -z^2/N$. Let us adopt the following notation for the expansion in λ:

$$\langle\psi|\psi\rangle = \sum_{n=0}^{N} \lambda^n P_n \quad (22)$$

P_0 has all of its factors arising from the bilinear (free) part of the Hamiltonian and is easily calculated. Performing the integrations yields

$$P_0 = z^{-N}\left\{\prod_{s<0}\prod_{t<0}\left[z^2 + 4\sin^2\left(\frac{2\pi s}{L}\right) + 4\sin^2\left(\frac{2\pi t}{L}\right)\right]\right\}^4 \quad (23)$$

Taking the logarithm of the above expression and replacing the resulting summations (in the large-N limit) with integrals provides

$$\ln[P_0] = -N\ln z + \frac{N}{\pi^2}\int_0^\pi dk_x \int_0^\pi dk_y \ln(z^2 + 4\sin^2 k_x + 4\sin^2 k_y) \quad (24)$$

Expanding the logarithm and integrating gives

$$\ln[P_0] = N\left[\ln(z^2+4) - \ln z - 2\sum_{n=1}^{\infty} \frac{1}{2n(z^2+4)^{2n}}\binom{2n}{n}^2\right] \quad (25)$$

The third term above can be reexpressed as

$$\sum_{n=1}^{\infty} \frac{1}{2n(z^2+4)^{2n}}\binom{2n}{n}^2 = \frac{2}{\pi}\int_0^{4/(z^2+4)} dk \, \frac{F(k,\pi/2) - \pi/2}{k} \quad (26)$$

where $F(k, \pi/2)$ is a complete elliptic integral of the first kind.

The constituents of P_1 have the $a_k^* a_p b_q^* b_{k+q-p}$ contribution from the expanded quartic portion, while all the rest arises from the free part of the Hamiltonian. The integral is nonzero only when $p = k$. After some manipulation one arrives at

$$P_1 = \left[\sum_{s>0}\sum_{t>0} \frac{4z}{z^2 + 4\sin^2(2\pi s/L) + 4\sin^2(2\pi t/L)}\right]^2 P_0 \quad (27a)$$

$$P_1 = \left[\frac{zN}{z^2+4} \sum_{n=0}^{\infty} (z^2+4)^{-2n} \binom{2n}{n}^2 \right]^2 P_0 \tag{27b}$$

$$P_1 = \left[\frac{zN}{z^2+4} \frac{2}{\pi} F\left(\frac{4}{z^2+4}, \frac{\pi}{2} \right) \right]^2 P_0 \tag{27c}$$

The constituents of P_2 are more complicated; they contain $a_k^* a_p a_r^* a_s b_q^* b_{k+q-p} b_t^* b_{r+t-s}$. The a_k^* may be paired (contracted) with a_p (if $k=p$), a_s (if $k=s$), or a_r^* (if $k=-r$); the b variables are contracted similarly. In addition, because the variables anticommute, k cannot equal r, and so forth. Consider the contribution to P_2 in which a_k^* is contracted with a_p, a_r^* with a_s, b_q^* with b_{k+q-p}, and b_t^* with b_{r+t-s} (call it $P_2^{(1)}$). An expression for $P_2^{(1)}$ follows:

$$P_2^{(1)} = \left[\frac{1}{2} \left(\sum_{s>0} \sum_{t>0} \frac{4z}{z^2 + 4\sin^2(2\pi s/L) + 4\sin^2(2\pi t/L)} \right)^2 - \sum_{s>0} \sum_{t>0} \frac{4z^2 - 16\sin^2(2\pi s/L)}{[z^2 + 4\sin^2(2\pi s/L) + 4\sin^2(2\pi t/L)]^2} \right]^2 P_0 \tag{28a}$$

$$P_2^{(1)} = \left\{ \frac{1}{2} \left[\frac{zN}{z^2+4} \frac{2}{\pi} F\left(\frac{4}{z^2+4}, \frac{\pi}{2} \right) \right]^2 - \frac{3}{2} \frac{z^2}{z^2+4} \frac{2}{\pi} \left[\frac{d}{dk} \left(kF\left(k, \frac{\pi}{2} \right) \right) \Big|_{k=4/(z^2+4)} \right] + \frac{1}{2} \frac{N}{z^2+4} \frac{2}{\pi} F\left(\frac{4}{z^2+4}, \frac{\pi}{2} \right) \right\}^2 P_0 \tag{28b}$$

There are six other contributions $P_2^{(i)}$, $i=2,\ldots,7$, to P_2 from the various "contractions" of the second-order term. These contributions, as well as all higher order terms, may conveniently be associated with corresponding Feynman diagrams and evaluated using Feynman rules.

Another possible perturbative approach would use the self-consistent solution to the decoupled Hamiltonian presented in Section 3.1 as its starting point. This procedure will coincide with a $1/n$ expansion.

3.3. Bounds on the Self-Overlap

In this section we present upper and lower bounds on $Z_N(2, 4)$. [Note that we have introduced a subscript N in expressions like $Z_N(2, 4)$ to indicate that the system contains N sites.] First, an upper bound on $Z_N(2, 4)$ is found in terms of $Z_N(1, 2)$. In a loop-dimer configuration, let l

be the total number of sites involved in loops. On a square lattice two relations among l, p, p_2, and N are easily seen:

$$2p_2 + l = N \tag{29}$$

$$p \leqslant l/4 \tag{30}$$

Combining these gives the following relation:

$$Z_N(2,4) = \sum_{\{C\}} 2^{p_2} 4^p \leqslant \sum_{\{C\}} 2^{p_2} 4^{l/4} = 2^{N/2} \sum_{\{C\}} 1 = 2^{N/2} Z_N(1,1) \tag{31a}$$

Unfortunately, a numerical expression for $Z_N(1,1)$ is not readily available. So, we must settle for a weaker bound in terms of $Z_N(1,2)$,

$$Z_N(2,4) \leqslant 2^{N/2} Z_N(1,1) \leqslant 2^{N/2} Z(1,2) \tag{31b}$$

$Z_N(2,4)$ and $Z_N(1,2)$ both grow exponentially with N; therefore, it is convenient to consider this inequality in terms of the "free energy" per site:

$$\frac{\ln[Z_N(2,4)]}{N} \leqslant \frac{\ln 2}{2} + \frac{2G}{\pi} \simeq 0.9297 \tag{31c}$$

Next, we set out to find lower bounds. The decoupling scheme produced $Z_N(1,2)$ as an approximation for $Z_N(2,4)$. One is readily convinced that $Z_N(1,2) \leqslant Z_N(2,4)$ for each involves a sum over the same configurations, with each configuration in $Z_N(1,2)$ having a smaller weight than it does in $Z_N(2,4)$. Therefore

$$\frac{\ln[Z_N(2,4)]}{N} \geqslant \frac{2G}{\pi} \simeq 0.5831 \tag{32}$$

Summing a subset of the weighted configurations will also produce a lower bound. For instance, among the configurations in $Z(2,4)$ are the close-packed dimer configurations with a factor of two per dimer. Consequently,

$$Z_N(2,4) \geqslant 2^{N/2} Z_{\text{dimer}} \tag{33a}$$

which implies

$$\frac{\ln[Z_N(2,4)]}{N} \geqslant \frac{\ln 2}{2} + \frac{G}{\pi} \simeq 0.6381 \tag{33b}$$

A better lower bound may, however, be extracted from considering $Z_N(2,4)$ on strips.[33] In the Appendix we show how the weighted

enumeration may be done exactly for a $2 \times Q$ strip and approximately for a $4 \times Q$ strip. From the latter we may extract a lower bound of 0.7321 [Eq. (A10)]. The free energy per site is thus bounded by

$$0.7321 \leqslant \frac{\ln[Z_N(2, 4)]}{N} \leqslant 0.9297 \tag{34}$$

4. FURTHER GENERALIZATIONS

So far we have considered a wavefunction which obeys the Marshall sign rule and which is therefore a candidate for the ground state of the half-filled system under certain conditions. What would be the excited states under the same conditions? One possibility is to consider states which are still superpositions of singlets, but with phases that do not satisfy the Marshall rule. We show how to incorporate such states into our framework. At the end of this section we also mention potential extensions to the presence of holes.

Let us define the pair of variables η^1, η^2 (and ξ^1, ξ^2) related to the previous ones by the transformation

$$\eta_i = \frac{1}{\sqrt{2}} (\eta_i^1 + i\eta_i^2) \tag{35a}$$

$$\eta_i^* = \frac{1}{\sqrt{2}} (\eta_i^1 - i\eta_i^2) \tag{35b}$$

Written in terms of these variables, the Hamiltonian [Eq. (10a)] is

$$H = \sum_i (\eta_i^1 \eta_{i+e_x}^1 + \eta_i^2 \eta_{i+e_x}^2) + i \sum_i (\eta_i^1 \eta_{i+e_y}^1 - \eta_i^2 \eta_{i+e_y}^2) + \{\eta \to \xi\} \tag{36}$$

The Hamiltonian may then be decoupled $H = H^{(1)}(\eta^1, \xi^1) + H^{(2)}(\eta^2, \xi^2)$. Note that $H^{(2)}(\rho, \lambda) = [H^{(1)}(\rho, \lambda)]^*$ if ρ and λ are "real" ($\rho^* = \rho$, $\lambda^* = \lambda$). It suggests that $\exp\{H^{(1)}\}$ provides the valence bonds associated with the ket $|\psi\rangle$ and $\exp\{H^{(2)}\}$ those associated with the bra $\langle\psi|$. The two species, however, remain coupled by the constraint, since the integration measure also changes:

$$d\eta_i^* \, d\eta_i \, d\xi_i^* \, d\xi_i (\xi_i^* \xi_i + \eta_i^* \eta_i) \to i \, d\eta_i^1 \, d\eta_i^2 \, d\xi_i^1 \, d\xi_i^2 (\eta_i^1 \eta_i^2 + \xi_i^1 \xi_i^2) \tag{37}$$

Next, we associate with each dimer, such as the one going from site i to the site $i + e_x$, a phase $\alpha_i(e_x)$. Accordingly, the singlet wavefunction becomes

$$\phi_{i, i+e_v} \to \phi_{i, i+e_v} \exp\{i\alpha_i(e_v)\} \tag{38}$$

Recalling that η^1, ξ^1 are related to kets and η^2, ξ^2 to bras, we see that the Hamiltonian is now given by

$$H = \sum_i \{\eta_i^1 \eta_{i+e_x}^1 \exp[i\alpha_i(e_x)] + \eta_i^2 \eta_{i+e_x}^2 \exp[-i\alpha_i(e_x)]\}$$
$$+ i \sum_i \{\eta_i^1 \eta_{i+e_y}^1 \exp[i\alpha_i(e_y)] - \eta_i^2 \eta_{i+e_y}^2 \exp[-i\alpha_i(e_y)]\} + \{\eta \to \xi\} \tag{39}$$

After performing the integration in $Z_G = \mathrm{Tr}(\exp H)$ over the η's and the ξ's, we find for the partition function

$$Z_G = \sum_{\{C\}} 2^{p_2} \prod_{\text{loops}} 4 \cos[\alpha_i(e_\nu) - \alpha_{i+e_\nu}(e_\mu) + \cdots - \alpha_{i-e_\tau}(e_\tau)] \tag{40}$$

where the configurations $\{C\}$ consist as before of double dimers and loops. The new feature is the cosine of the staggered phase sum along the loops.

The partition function at finite temperature would require the knowledge of the energy difference between the Marshall state (in which all phases are equal) and these excited states. We leave that for future investigations. We only note that this will yield an effective $U(1)$ gauge theory for the free energy similar to that derived by Baskaran and Anderson.[34] It is also clear that since the phase difference between all pairs of neighboring bonds around the loop may be made arbitrarily small, the low-lying excitations are gapless. These are precisely the "resonons" discussed by Rokhsar and Kivelson.[24]

In two dimensions the $U(1)$ gauge system is in its confining phase for all finite temperatures. Yet at $T=0$ the NNRVB "condenses" into the Marshall state. We expect the associated singularities in the thermodynamic functions to be of the type $\exp(-C/T)$, typical of a system below its lower critical dimension. (Another possibility found in the large-n limit[23] and in the quantum dimer model,[24] which also involves only the smallest loops, is that phase fluctuations stabilize the "spin-Peierls" state.)

More general RVB states may consist of singlet pairs between spins which are not necessarily nearest neighbors. One class of wavefunctions, suggested by Liang, Douçot, and Anderson (LDA), includes only pairs of spins belonging to the different sublattices. Their lengths are controlled by a variational weight function. Our approach is readily generalized to such LDA wavefunctions as well. The explicit diagonalization of the quadratic (nonconstrained) Hamiltonian will, however, contain the Fourier transform of the weight function explicitly and the low-momentum dispersion will be determined by its long-range decay. As for exact bounds on the partition function, they may be derived only for fairly simple weight functions.

We conclude this section with a few words on the effect of dilution. First, if we consider only static holes (or vacancies), the Marshall rule still applies. Read and Chakraborty[35] have shown that a flux of a half quantum should be associated with each hole in order to satisfy the relation between the sign and the area enclosed by the loop. This may be realized by changing the signs of all bonds along a string which extends from the plaquette adjacent to the hole up to infinity (or to a hole on the opposite sublattice, if present). So static holes may be incorporated in the present formalism without much difficulty.[15] The real challenge is to allow for moving holes. The motion of the holes is another source of frustration. The phases on the dimers then must be correlated with the motion of the holes. This may lead to generalized flux phases.[6,36,37] Different ways to incorporate these effects into the formalism are currently being investigated.

5. CONCLUSION

Let us summarize our achievements in the present work. First, we have demonstrated how the overlap of the NNRVB wavefunction may be expressed as the trace of a Hamiltonian composed of a sum of bilinear (bond) terms of classical anticommuting (Grassmann) variables. As stated in the Introduction, this is a very desirable outcome in view of the fact that the underlying particles carrying the spins are electrons (namely fermions). The constraint of one electron per site was imposed by the redefinition of the Grassmannian integration measure. However, the constraint-imposing term may also be absorbed in the action as a local "potential." We showed that the corresponding vertex consists of one term for every site which is a product of the four anticommuting variables.

In order to deal with such an interaction, we have initiated two approaches: one is a systematic perturbation expansion around the constraint-free, quadratic (and hence soluble) theory. The other approach is nonperturbative and relies on a self-consistent decoupling of the quadratic term (à la Hartree–Fock).

As the next step, we shall address the dimer–dimer correlations in this state. It has been conjectured by Sutherland[22] that they exhibit a power-law decay. It would be desirable to be able to confirm this prediction and, if so, to provide a renormalization scheme to estimate the associated power law. The answer to this question is of importance, since this algebraic decay of dimer–dimer correlations may turn out to be one of the most important characteristics of the "featureless" spin-liquid RVB state.

We have outlined the first step toward implementing into the formalism phase fluctuations, dilution with static and moving holes, and the

parity-violating flux phases. So this approach has the promise to be a useful framework for the future study of wavefunctions of strongly interacting electronic systems.

APPENDIX

We will consider here a method for calculating $Z_N(2, 4)$ on a strip and then employ these results to find lower bounds on $Z_N(2, 4)$ in 2D. Consider a $P \times Q$ lattice; such a lattice can be divided into P/W strips of dimension $W \times Q$. One can derive a lower bound by summing the subset of configurations in which no bonds connect sites belonging to different strips. We have

$$Z_{P\times Q}(2, 4) \geqslant [Z_{W\times Q}(2, 4)]^{P/W} \tag{A1a}$$

or, written in terms of the "free energy" per site,

$$\frac{\ln[Z_{P\times Q}(2, 4)]}{PQ} \geqslant \frac{\ln[Z_{W\times Q}(2, 4)]}{QW} \tag{A1b}$$

Consider classifying the configurations contributing to $Z_{W\times Q}(2, 4)$ on a strip in the following way: Begin at the left of the strip and find the first place at which one can draw a vertical line without cutting through any bonds. If the line can be drawn between the first and second positions, the configuration belongs to the first class; if it falls between the second and third positions, the configuration belongs to the second class, and so forth. Next notice that the contribution due to the nth class is a product of two terms: (1) the weighted configurations belonging to $Z_{W\times n}(2, 4)$ through which no vertical lines can be drawn (call this C_n) and (2) $Z_{W\times(Q-n)}(2, 4)$ (it does not matter what happens beyond the nth position). The following relation then holds:

$$Z_{W\times Q}(2, 4) = C_1 Z_{W\times(Q-1)}(2, 4) + C_2 Z_{W\times(Q-2)}(2, 4) + \cdots + C_W Z_0(2, 4) \tag{A2}$$

If W is even, then C_1 equals $2^{W/2}$; if it is odd, then C_1 equals zero.

The case $W = 2$ is particularly simple.[32] $Z_{2\times Q}(2, 4)$ obeys the following recursion relation:

$$\begin{aligned} Z_{2\times Q}(2, 4) = {} & 2Z_{2\times(Q-1)}(2, 4) + 8Z_{2\times(Q-2)}(2, 4) + 4Z_{2\times(Q-3)}(2, 4) \\ & + 4Z_{2\times(Q-4)}(2, 4) + \cdots + 4Z_{2\times 1}(2, 4) + 4Z_0(2, 4) \end{aligned} \tag{A3}$$

where $Z_0(2, 4) = 1$ and $Z_{2\times 1}(2, 4) = 2$. C_1 is two—corresponding to a vertical dimer; C_2 is eight—corresponding to a pair of horizontal dimers and a

loop (each with a weight of four). All the rest are four because there is only one contributing diagram—a loop of length $(n-1)$.

Now assume that $Z_{2\times Q}(2,4)$ can be expressed as f^Q and place this into the recursion relation. We have

$$f^Q = 2f^{Q-1} + 8f^{Q-2} + 4f^{Q-3}\sum_{n=0}^{Q-3} f^{-n} \tag{A4}$$

The sum is a geometric series and easily solved. After eliminating small terms, the recursion relation yields

$$f^3 - 3f^2 - 6f + 4 = 0 \tag{A5}$$

The root of interest is $f \simeq 4.2015$. Utilizing the expression in Eq. (A1b), one can conclude

$$\frac{\ln[Z_{P\times Q}(2,4)]}{PQ} \geqslant \frac{\ln f}{W} \simeq 0.7177 \tag{A6}$$

The coefficients in the case of a wider strip are more difficult to obtain. However, instead of calculating all of the coefficients, one can calculate the first few and write expression (A3) as an inequality:

$$Z_{W\times Q}(2,4) \geqslant C_1 Z_{W\times(Q-1)}(2,4) + \cdots + C_n Z_{W\times(Q-n)}(2,4) \tag{A7}$$

For instance, in the case W equals four, one obtains the following relation:

$$Z_{4\times Q}(2,4) \geqslant 4Z_{4\times(Q-1)} + 180Z_{4\times(Q-2)} + 960Z_{4\times(Q-3)} + 12152Z_{4\times(Q-4)} \tag{A8}$$

One can improve this relation by selecting a conveniently summable subset of configurations contributing to the rest of the C_n. For instance, consider those configurations of length n in which a vertical line would pass through either a pair of horizontal dimers separated by a single lattice spacing or through a square the size of a plaquette. (A single vertical bond will appear on each end.) A typical configuration for $n=6$ is shown in Fig. 4. For this subset C'_n equals 8^n. The relation then becomes

$$\begin{aligned} Z_{4\times Q}(2,4) \geqslant{}& 4Z_{4\times(Q-1)} + 180Z_{4\times(Q-2)} + 960Z_{4\times(Q-3)} \\ &+ 12152Z_{4\times(Q-4)} + \sum_{n=5}^{Q} 8^n Z_{Q-n} \end{aligned} \tag{A9}$$

Expressing $Z_{4\times Q}(2,4)$ as g^Q leads to

$$g^5 - 12g^4 + 148g^3 + 480g^2 - 4472g + 64448 = 0$$

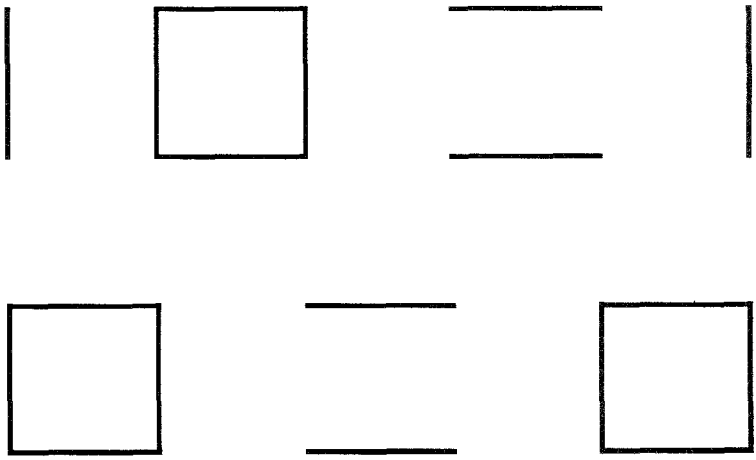

Fig. 4.

The relevant root is $g \simeq 18.6989$, which implies

$$\frac{\ln[Z_{P\times Q}(2,4)]}{PQ} \geqslant \frac{\ln g}{4} \simeq 0.7321 \tag{A10}$$

It would be straightforward, though very cumbersome, to pursue this method of bettering the lower bound.

ACKNOWLEDGMENTS

Part of the work by one of us (Y. S.) was performed during a stay at the Technion as a Compton visiting fellow. Gratitude is expressed to the Compton Foundation for its support and to S. Fishman for his warm hospitality. Discussions and bitnet correspondence with M. Kohmoto are also acknowledged.

REFERENCES

1. P. W. Anderson, The resonating valence bond state in La_2CuO_4 and superconductivity, *Science* **235**:1196 (1987).
2. G. Baskaran, Z. Zou, and P. W. Anderson, The resonating valence bond state and high T_c superconductivity—A mean field theory, *Solid State Commun.* **63**:973 (1987).
3. I. Affleck and J. B. Martson, Large-n limit of the Heisenberg–Hubbard model: Implications for high-T_c superconductors, *Phys. Rev. B* **37**:3774 (1988).
4. G. Kotliar, Resonating valence bond and d-wave superconductivity, *Phys. Rev. B* **37**:3664 (1988).

5. S. Kivelson, D. Rokhsar, and J. Sethna, Topology of the resonating valence-bond state: Solitons and high-T_c superconductivity, *Phys. Rev. B* **35**:8865 (1987).
6. X. G. Wen, F. Wilczek, and A. Zee, Chiral spin states and superconductivity, *Phys. Rev. B* **39**:11413 (1989).
7. T. Holstein and H. Primakoff, Field dependence of the intrinsic domain magnetization of a ferromagnet, *Phys. Rev.* **58**:1098 (1940).
8. P. W. Anderson, An approximate quantum theory of the antiferromagnetic ground state, *Phys. Rev.* **86**:694 (1952).
9. C. Kittel, *Quantum Theory of Solids* (Wiley, New York, 1963).
10. F. D. M. Haldane, Continuum dynamics of the 1-D Heisenberg antiferromagnet: identification with the $O(3)$ nonlinear sigma model, *Phys. Lett.* **93A**:464 (1983).
11. P. W. Anderson, *Mater. Res. Bull.* **8**:153 (1973). P. Fazekas and P. W. Anderson, On the ground state properties of the anisotropic triangular antiferromagnet, *Philos. Mag.* **30**:423 (1974).
12. H. Bethe, *Z. Phys.* **71**:205 (1931).
13. L. Hulthèn, *Ark. Mat. Astr. Fys.* **26A**:1 (1938).
14. A. Liang, B. Douçot, and P. W. Anderson, Some new variational resonating-valence-bond-type wave functions for the spin-1/2 antiferromagnetic Heisenberg model on a square lattice, *Phys. Rev. Lett.* **61**:365 (1988).
15. Y. Shapir, The Néel-RVB transition upon doping with static holes, ITP preprint (1989).
16. H. Tasaki, Order and disorder in the resonating-valence-bond state, preprint.
17. B. Sutherland, Systems with resonating valence bond ground states: Correlations and excitations, *Phys. Rev. B* **37**:3786 (1988).
18. M. Kohmoto and Y. Shapir, Antiferromagnetic correlations of the resonating valence bond state, *Phys. Rev. B* **37**:9439 (1988).
19. Y. Shapir and M. Kohmoto, Exact mapping of the resonating valence bond state to a classical $O(4)$ model in a logarithmic potential: Mean field theory, magnetic correlations and excitations, *Phys. Rev. B* **39**:4524 (1989).
20. W. Marshall, Antiferromagnetism, *Proc. R. Soc. Lond. A* **232**:48 (1955).
21. B. Sutherland, Monte Carlo investigation of the resonating-valence-bond ground state and a lattice statistical model, *Phys. Rev. B* **38**:6855 (1988).
22. B. Sutherland, The phase diagram of a lattice statistics problem associated with the resonating valence bond ground state, preprint.
23. N. Read and S. Suchdev, Valence-bond and spin-Peierls states of low-dimensional quantum antiferromagnets, *Phys. Rev. Lett.* **62**:1694 (1989).
24. D. Rokhsar and S. Kivelson, Superconductivity and the quantum hard core dimer gas, *Phys. Rev. Lett.* **61**:2376 (1988).
25. E. Lieb, T. Schultz, and D. Mattis, Two soluble models of an antiferromagnetic chain, *Ann. Phys.* (N. Y.) **16**:407.
26. P. Jordan and E. Wigner, Über das Paulische Äquivalenzverbot, *Z. Phys.* **47**:631 (1928).
27. E. Fradkin, Jordan–Wigner transformation for quantum spin systems in two dimensions and fractional statistics, *Phys. Rev. Lett.* **63**:322 (1989).
28. Y. Shapir and T. Blum, Grassmannian approach to the RVB state of the 2D Heisenberg antiferromagnet, *Mod. Phys. Lett.* **3**:925 (1989).
29. Y. Shapir, Supersymmetric statistical models on the lattice, in *Physica D* **15**:129 (1985).
30. S. Samuel, The use of anticommuting variable integrals in statistical mechanics. I. The computation of partition functions, *J. Math. Phys.* **21**:2806 (1980).
31. S. Samuel, The use of anticommuting variable integrals in statistical mechanics. III. Unsolved models, *J. Math. Phys.* **21**:2820 (1980).
32. P. W. Kasteleyn, The statistics of dimers on a lattice, *Physica* **27**:1209 (1961).

33. Y. Fan and M. Ma, Generating-function approach to the resonating-bond state on the triangular and square ladders, *Phys. Rev. B* **37**:1820 (1988).
34. G. Baskaran and P. W. Anderson, Gauge Theory of high-temperature superconductors and strongly correlated Fermi systems, *Phys. Rev. B* **37**:580 (1988).
35. N. Read and C. Chakraborty, Statistics of the excitations of the resonating valence bond state, *Phys. Rev. B* **40**:7133 (1989).
36. V. Kalmeyer and R. B. Laughlin, Equivalence of the resonating valence bond and fractional quantum Hall states, *Phys. Rev. Lett.* **59**:2095 (1987).
37. R. B. Laughlin, The relationship between high-temperature superconductivity and the fractional Quantum hall effect, *Science* **242**:525 (1988).